

Delayed formation of Arctic snow cover in response to wildland fires in a warming climate

Received: 16 October 2024

Accepted: 22 August 2025

Published online: 23 September 2025

Yamin Qing^{1,2,8}, Shuo Wang^{1,2,3,8}✉, Amir AghaKouchak^{4,5,6} & Pierre Gentine⁷

Wildland fires in seasonally snow-covered areas can have lasting effects on both the snowpack and carbon stocks. Here, using long-term satellite data, we show that from 1982 to 2018, the burned area in the Arctic has significantly increased, while the duration of snow cover has significantly decreased. An XGBoost machine learning model and causal analysis confirmed the role of wildland fires in delaying snow cover formation, with this effect strongly linked to fire-induced reductions in albedo and increases in temperature. In addition, we observed a delay of more than 5 days in snow cover formation following major wildland fires. Looking ahead, our projections under a high-emissions scenario (Shared Socioeconomic Pathway, SSP 5-8.5) indicate that the burned area could increase by a factor of 2.6 and the annual mean snow cover duration could decrease by nearly 18 days between 2015 and 2100 compared with the historical average.

Snow cover in the Arctic region (latitude $\geq 60^\circ$ N) plays an important role in the global climate system, notably impacting the hydrological cycle^{1–4}, global energy balance and weather patterns^{2,5,6}. However, climate change is anticipated to cause a shift in snowpack, leading to later formation or earlier melting^{7–9}. This shift could reduce snow-dominated water resources and broadly impact freshwater supply^{1,10}, ecosystem productivity¹¹, agricultural irrigation¹², groundwater recharge¹³, food security^{14,15} and hydrological extremes^{16,17}.

Meanwhile, wildland fires are increasingly prevalent in the Arctic, with their size, frequency and intensity expected to rise as the climate warms^{18–21}. Notably, in 2023, a record-breaking fire season burned over 45 million acres in Canada, almost ten times the 1983–2022 annual average burned area (BA) of 5.2 million acres (Canadian Interagency Forest Fire Centre). In addition, in the summer of 2022, wildland fires impacted more than 1.2 million acres across southwestern Alaska²². Wildfires also scorched areas along the Arctic Circle, incinerating

tundra and blanketing Siberian regions with smoke²³. Furthermore, fires occurring in snow-covered areas could modify snow accumulation, ablation and duration, exacerbating the subsequent impacts of reduced snow cover. Thus, wildland fires in snow-covered areas are concerning as a result of the long-lasting impacts they can have on the snowpack, particularly in the Arctic region.

Given the anticipated reductions in snow cover and increased severity of wildland fires under a warmer Arctic climate, it is essential to consider their interaction, particularly how snow cover responds to intensified wildland fires. The importance of this stems from evidence that wildland fires can modify snow characteristics, although the sign and magnitude of these impacts can substantially vary across different regions^{24,25}. For instance, observations across the western United States indicate that a decline in peak snow after a fire is more common²⁶, probably due to fire-related changes to the snowpack energy balance²⁷. As previous studies on snow cover and wildland fires have not considered

¹State Key Laboratory of Climate Resilience for Coastal Cities (SKL-CRCC), The Hong Kong Polytechnic University, Hong Kong, China. ²Department of Land Surveying and Geo-Informatics, The Hong Kong Polytechnic University, Hong Kong, China. ³Research Institute for Land and Space and Research Institute for Sustainable Urban Development, The Hong Kong Polytechnic University, Hong Kong, China. ⁴Department of Civil and Environmental Engineering, University of California, Irvine, CA, USA. ⁵Department of Earth System Science, University of California, Irvine, CA, USA. ⁶United Nations University, Institute for Water, Environment and Health, United Nations University, Hamilton, Ontario, Canada. ⁷Department of Earth and Environmental Engineering, Columbia University, New York, NY, USA. ⁸These authors contributed equally: Yamin Qing, Shuo Wang. ✉e-mail: shuo.s.wang@polyu.edu.hk

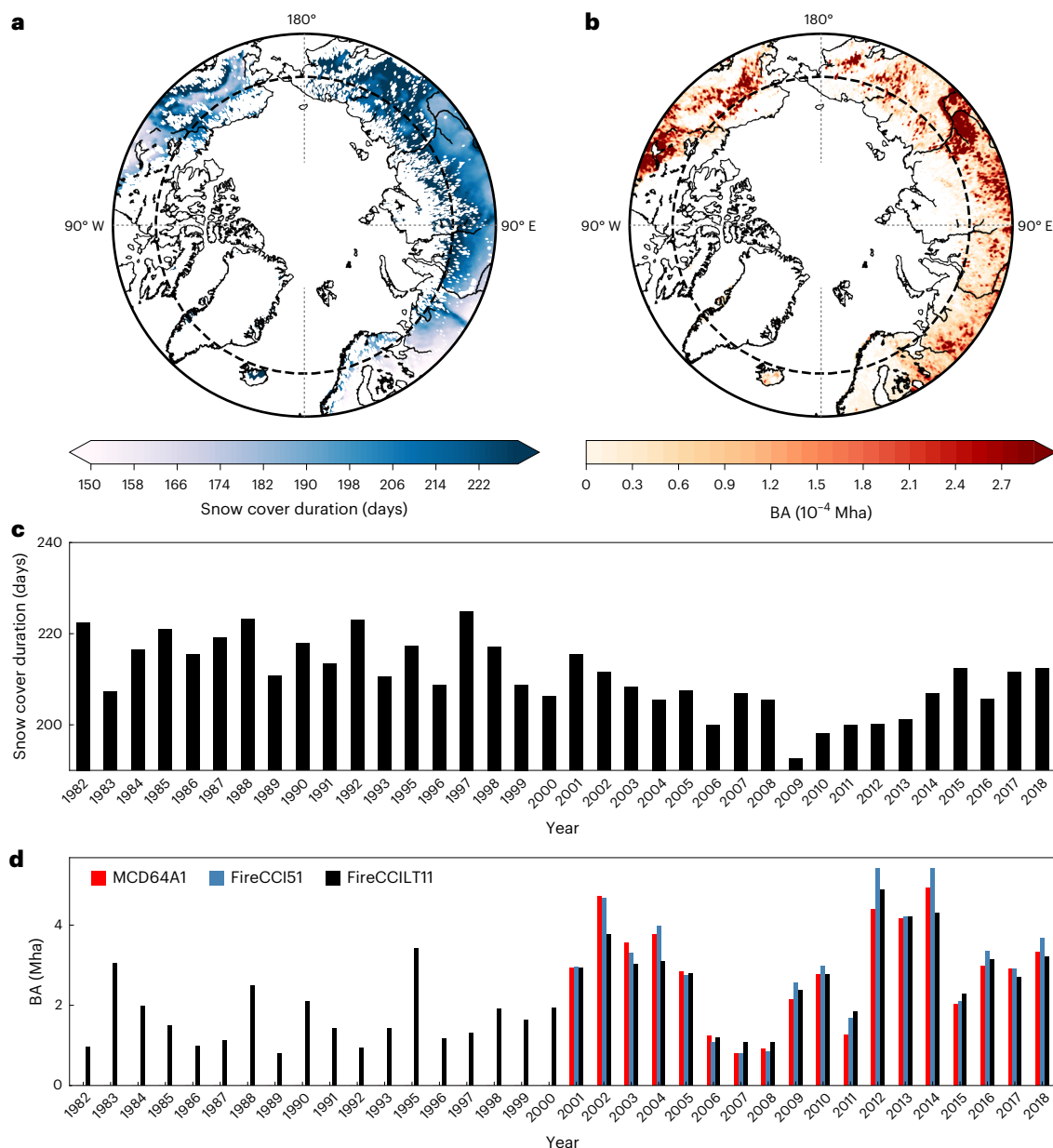


Fig. 1 | Spatiotemporal changes in snow cover and BA for 1982–2018 over the Arctic region. **a**, Extent of the annual mean snow cover duration over areas that experienced wildland fire from 1982 to 2018. **b**, Extent of the burns for 1982–2018 from the FireCCILT11 product. **c**, Annual snow cover duration over areas that experienced wildland fire from 1982 to 2018. **d**, Annual BA in the Arctic region, derived from three products (FireCCI51, MCD64A1 and FireCCILT11).

Satellite BA products do not contain data for 1994 and the data for 1994 in daily snow data are also removed. Basemaps in **a** and **b** from Natural Earth (<https://www.naturalearthdata.com/>), generated with matplotlib with geospatial data from GSHHG (<https://www.soest.hawaii.edu/pwessel/gshhg/>) under a Creative Commons licence **CC0**.

their interplay, it remains largely unknown whether and how major wildland fires might reduce the duration of snow cover in the Arctic region.

We used three satellite-based BA products (FireCCILT11, FireCCI51 and MCD64A1) and a daily gridded snow water equivalent (SWE) reconstruction for the recent decades (1982–2018) to assess changes in BA and snow cover, as well as their interactions in the Arctic region (Methods). We developed XGBoost (extreme gradient boosting) models incorporating a range of climate factors—including albedo, land surface temperature (LST), air temperature (T_a), vapour pressure deficit (VPD), surface downwelling shortwave flux (SW), surface downwelling longwave flux (LW) and climatic water deficit (Def)—across pre-fire, during-fire and post-fire phases. We also included summertime BA, latitude and longitude to analyse the contribution of all factors to changes in snow cover duration. In addition, we used causal analysis to

investigate the causal effects of wildland fires on snow cover changes. The response of snow cover duration to major wildland fires was then assessed. Last, we examined the trends in wildland fires and snow cover under three future Shared Socioeconomic Pathways (SSPs 2-4.5, 3-7.0 and 5-8.5) from the Coupled Model Intercomparison Project phase 6 (CMIP6) simulations.

Trends in BA and snow cover

We begin with a broad overview of changes in annual snow cover duration (limited to snow-covered areas where wildland fires have occurred) and BA from 1982 to 2018. Generally, annual snow cover duration increases with latitude. The longest duration, exceeding 220 days, occurs within the Arctic Circle, while the shortest duration, typically less than 150 days, is observed south of the Arctic Circle (Fig. 1a).

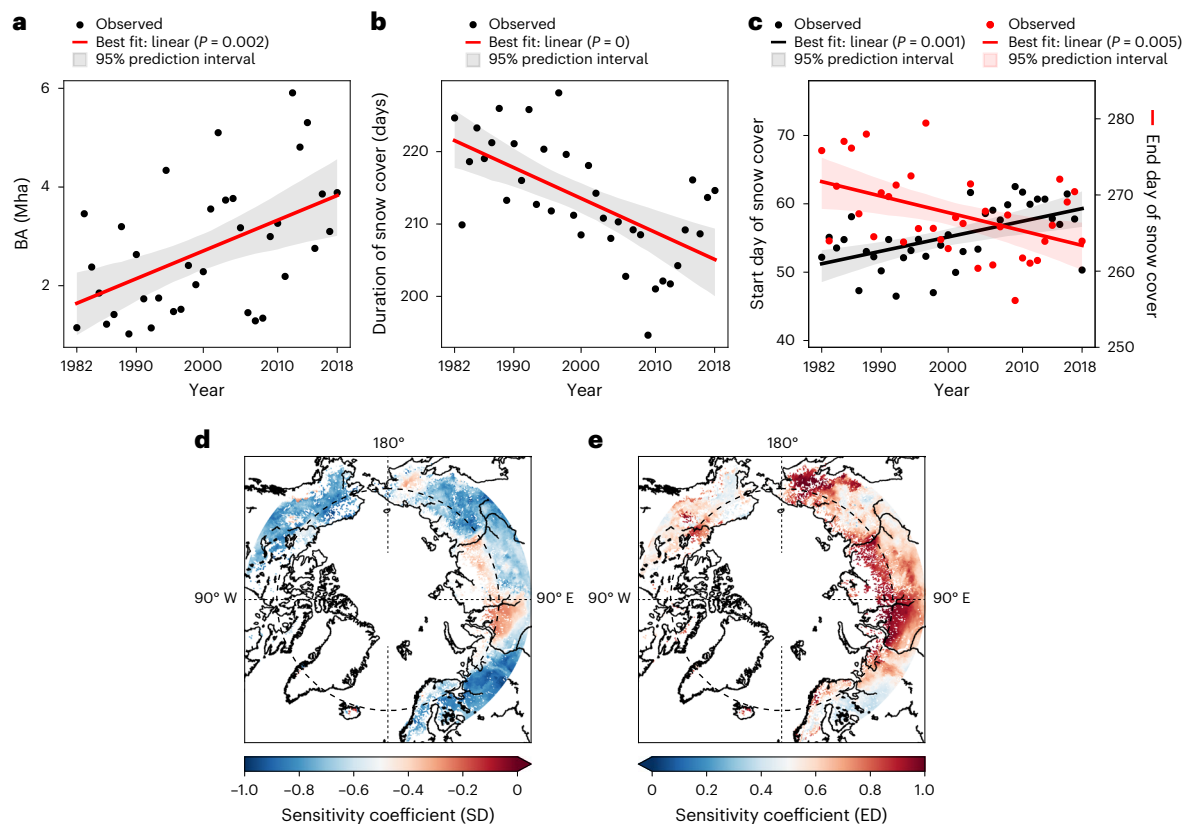


Fig. 2 | Changes in snow cover phenology and BA across the Arctic from 1982 to 2018. **a**, Trend in annual BA (Mha) based on FireCCILT11. **b**, Trend in annual snow cover duration (days) over areas affected by wildland fire. **c**, Trends in the start (black) and end (red) dates of snow cover over fire-affected areas. In **a–c**, trends are estimated using least-squares linear regression over the 1982–2018 period and statistical significance is assessed using two-sided *t*-tests with *P* values derived from the regression model. **d**, Spatial sensitivity of SD to

changes in snow cover duration over the 1982–2018 period. **e**, Spatial sensitivity of ED to changes in snow cover duration over the 1982–2018 period. Panels **d** and **e** show only regions with statistically significant results based on multiple linear regression. Basemaps in **d** and **e** from Natural Earth (<https://www.naturalearthdata.com/>), generated with matplotlib with geospatial data from GSHHG (<https://www.soest.hawaii.edu/pwessel/gshhg/>) under a Creative Commons licence CC0.

On the other hand, the satellite-based BA product FireCCILT11 captures the widespread fire activity that has occurred across the Arctic region (Fig. 1b). Furthermore, snow cover duration has decreased across the Arctic region from 1982 to 2018 (Fig. 1c). Quantitatively, from 2001 to 2018, the average snow cover duration was 205 days, which is 10 days shorter than the 1982–2000 average. Meanwhile, although BA estimates in the Arctic region vary among satellite BA products, all have shown an increasing trend, with the most pronounced rise observed in the FireCCILT11 product (Fig. 1d). The mean BAs estimated by FireCCILT11, FireCCI51 and MCD64A1 from 2001 to 2018 were 2.8 Mha, 3.0 Mha and 2.9 Mha, respectively. These values are 1.6, 1.8 and 1.7 times greater than the mean BA estimated by FireCCILT11 for the period 1982 to 2000.

The annual BA in the Arctic region has shown a significant increasing trend ($P < 0.01$), with an increase of approximately 2 Mha (Fig. 2a), particularly during 2010–2018, when the levels were higher than those observed in 2001–2009 (Supplementary Fig. 1). Meanwhile, in areas affected by wildland fires, snow cover duration exhibited a significant decreasing trend ($P < 0.01$), shortening by more than 15 days over the study period, with a similar decline observed over the past approximately two decades (Fig. 2b and Supplementary Fig. 1). Notably, in the Arctic, the snow cover formation date showed a substantial delay (indicating later snow cover formation), while the snow end date advanced (indicating earlier snowmelt), both of which are consistent with climate warming (Fig. 2c). Specifically, delayed snow cover formation was more pronounced below the Arctic Circle, while earlier snowmelt was more evident above it (Fig. 2d,e). These patterns suggest that the

shortening of the snow season may be associated with warming during early winter and spring.

Effect of wildland fires on snow cover

To assess whether delayed snow cover formation and early disappearance are linked to pre-snow-season wildland fires, we first analysed the factors influencing changes in snow cover from 1982 to 2018. Delayed snow cover formation and early disappearance were defined as snow start and end dates (SD and ED) deviating by more than 1 s.d. from the mean. We trained XGBoost models to predict annual delayed snow cover formation and early disappearance using climatic variables (albedo, LST, T_a , VPD, SW, LW and Def) across pre-fire, during-fire and post-fire phases, along with summertime BA, latitude and longitude. The models performed well ($F_2 = 0.82$, recall = 0.96), outperforming other machine learning methods (Supplementary Fig. 2 and Supplementary Table 1) and their interpretability revealed key drivers. As shown in Fig. 3a, post-fire factors had the strongest influence on delayed snow cover formation, consistent across different spatial resolutions (Supplementary Fig. 3). Furthermore, post-fire albedo, T_a and LST were the most important predictors. Some larger BA values were also associated with higher Shapley additive explanation (SHAP) values, particularly under conditions of higher post-fire T_a , lower post-fire albedo and higher post-fire LST. This indicates that delayed snow cover formation is more sensitive to post-fire warming and surface darkening in areas affected by severe summer fires (Fig. 3b,c and Supplementary Fig. 4). However, albedo, LST, T_a , VPD, SW, LW and Def across the pre-fire, during-fire and post-fire phases, as well as BA, latitude and longitude,

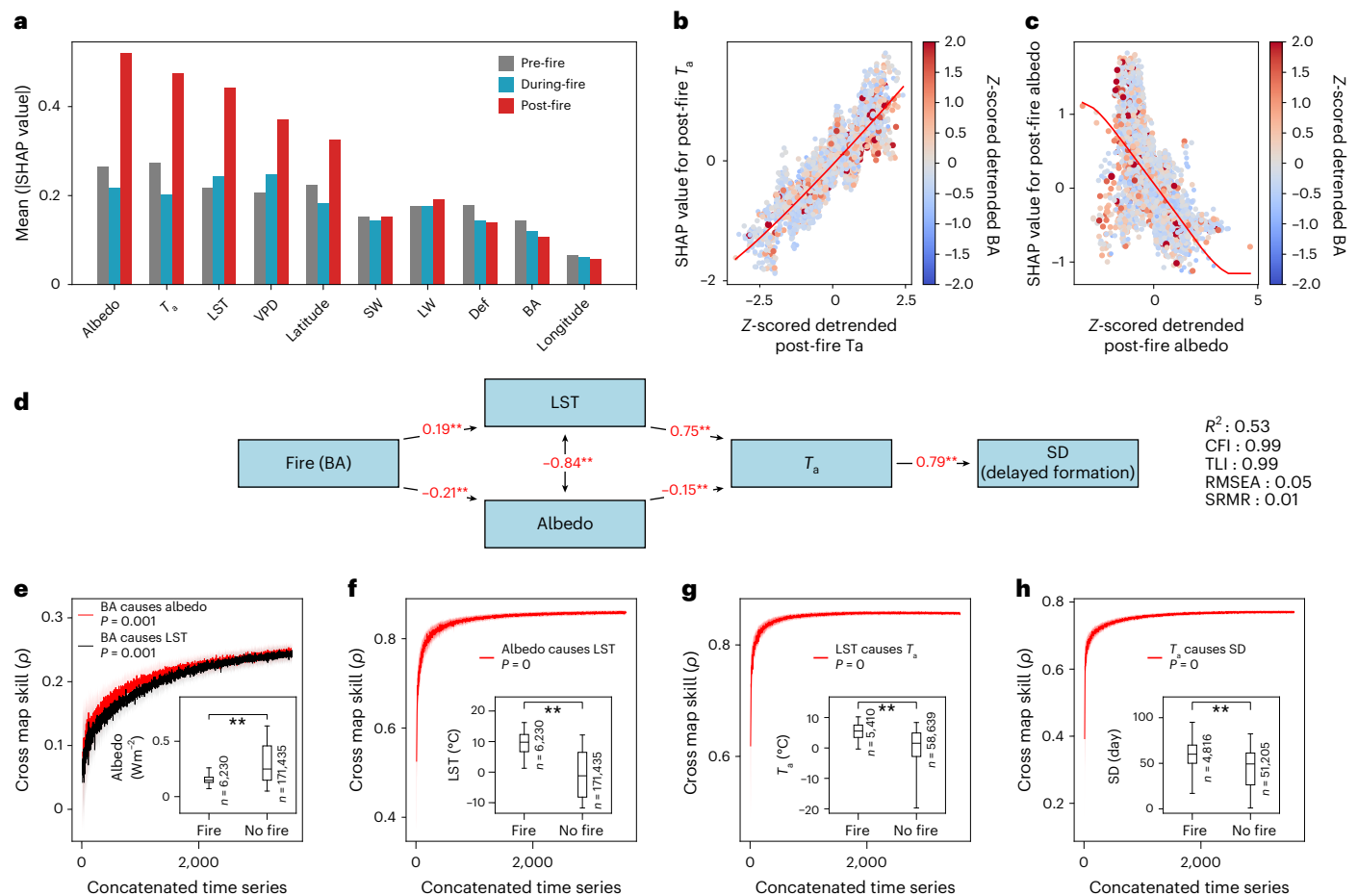


Fig. 3 | Machine learning and causal analyses of the drivers of delayed snow cover formation following fire events. **a**, Mean SHAP values for various variables (albedo, T_a , LST, VPD, SW, LW and Def) during the pre-fire (grey), during-fire (blue) and post-fire (red) periods, with BA, latitude and longitude. Values are computed in 8×8 grid boxes (that is, $2^\circ \times 2^\circ$) using the XGBoost model. **b, c**, SHAP dependence plots for post-fire T_a (**b**) and post-fire albedo (**c**), respectively, with colour indicating BA. Red lines indicate fitted trends. **d**, SEM illustrating causal relationships between summertime fire, post-fire albedo, post-fire LST, post-fire T_a and SD. Standardized path coefficients are shown along arrows; significance is indicated (** $P < 0.01$). **e–h**, Causal relationships between summertime BA, post-fire albedo (**e**), post-fire LST (**f**), post-fire T_a (**g**) and SD (**h**) based on the CCM

are not sufficiently significant in explaining early snow cover disappearance (Supplementary Fig. 5).

We then used structural equation modelling (SEM) to explore the potential mechanisms underlying the substantially delayed snow response to wildland fires, with a particular focus on the key roles of post-fire albedo, LST and T_a (Fig. 3d). We found that summertime BA significantly increased post-fire LST and simultaneously decreased post-fire albedo, with path coefficients of 0.19 and -0.21 , respectively. The reduction in post-fire albedo further increased LST (-0.84 , $P < 0.01$) and the rise in LST significantly elevated T_a , with a path coefficient of 0.75 ($P < 0.01$), ultimately leading to delayed snow cover formation ($R^2 = 0.53$, $P < 0.01$). This pathway remained robust across different spatial resolutions (Supplementary Fig. 6). In addition, each pathway in the SEM was validated using convergent cross mapping (CCM). BA significantly influenced post-fire LST and post-fire albedo ($\rho = 0.21$ and 0.22), with post-fire conditions showing higher LST and lower albedo compared with non-fire years (Fig. 3e). Causal links were also confirmed from albedo to LST and from LST to T_a (Fig. 3f,g). Post-fire T_a strongly influenced delayed snow cover formation ($\rho = 0.78$, $P < 0.05$),

model, applied in 8×8 grid boxes ($2^\circ \times 2^\circ$). The x axis shows the concatenated time series across all grid boxes. Shaded areas indicate the mean \pm s.d. from 1,000 bootstrapped iterations. Insets in e–h show box plots comparing variable values between fire and non-fire years (** $P < 0.01$). The short horizontal line inside the box represents the 50th percentile and the top and bottom edges of the box represent the 75th and 25th percentiles, respectively. The upper and lower ends of the whiskers represent the 95th and 5th percentiles, respectively. The P value (** $P < 0.01$) from the two-sided Kolmogorov–Smirnov test, which was used to assess the statistical difference between the bias distributions of the two categories, is shown at the top centre of insets in e–h.

indicating that fire drives delays in snow cover formation (Fig. 3h). This CCM remained robust across different spatial resolutions (Supplementary Fig. 7).

In the Arctic, the primary ecosystem is tundra^{28,29}. However, charred tundra has a lower albedo than unburned areas, absorbing more solar radiation and thereby increasing LSTs³⁰. Fire amplifies this effect through both direct heating and the reduction of surface albedo, further warming the ground and increasing T_a . In the post-fire phase, especially during late autumn and early winter, these warmer conditions hinder snow accumulation, resulting in delayed snow cover formation (Supplementary Fig. 8). Overall, the delay in snow cover formation becomes more pronounced with increasing wildland fires and the associated post-fire warming.

Response of snow cover to major fires

We further examined the regional response of snow cover (SD and ED) to major wildland fires in the Arctic using the widely adopted superposed epoch analysis (SEA), also known as compositing. Major wildland fires were defined as those with a total annual BA of >1 s.d.

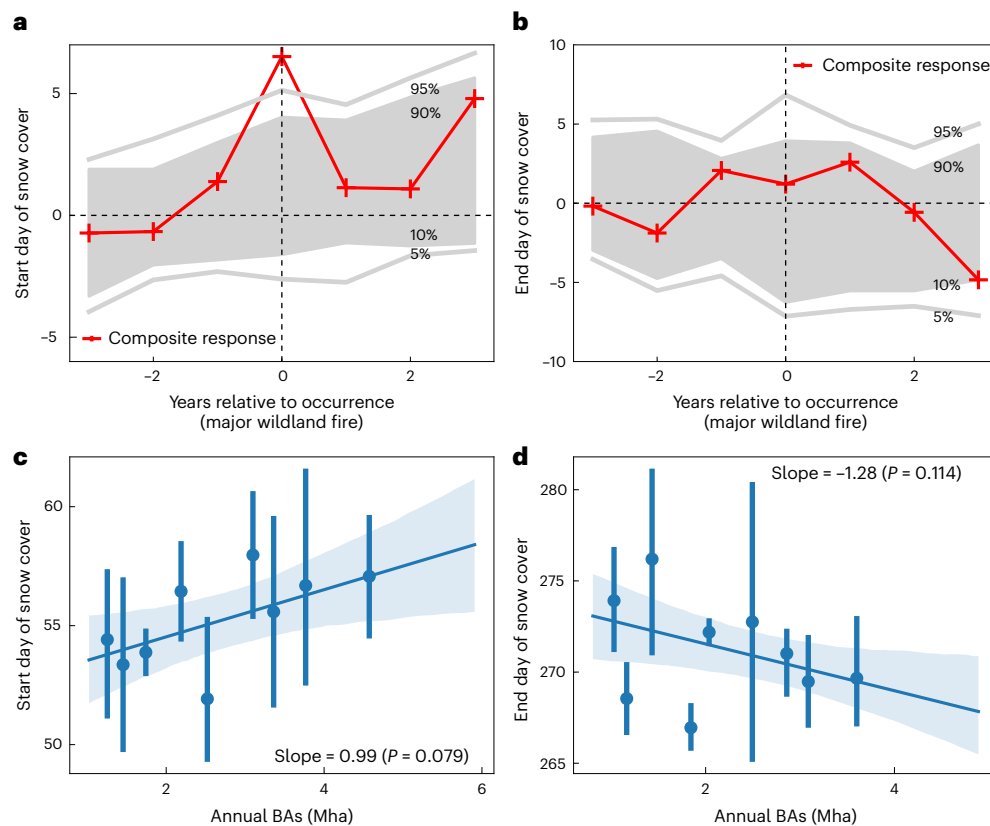


Fig. 4 | Response of the start and end days of snow cover to major wildland fires from 1982 to 2018 across the Arctic region. a, SEA showing the SD in response to major wildland fires. **b**, SEA showing the ED in response to major wildland fires. The horizontal lines in **a** and **b** indicate the threshold required for epochal anomalies to be statistically significant using random 1,000-bootstraping. **c**, BA-dependent amplification of the SD. **d**, BA-dependent amplification of

the ED. In **c** and **d**, the regression is based on the spatial domain and the shaded area surrounding the regression lines represents the 90% CI of regression estimates. The blue markers and error bars show the mean percentage change at different BA categories and their 90% CI. The blue markers and lines are drawn at the midpoint of each category. In **c** and **d**, P values are based on the two-sided Student's t -test.

above the mean during the 1982–2018 period. Our SEA results show a significant delay ($P < 0.05$) in the snow cover start date in the years following major fire events in the Arctic (Fig. 4a). This finding remains consistent across different thresholds used to define major wildland fires and is further supported by an increased sample size for robust event detection using bootstrap resampling with noise (Supplementary Figs. 9 and 10). The most pronounced delay—exceeding 5 days relative to the 3-year pre-fire average—occurs in the snow year immediately following fire events. Bootstrapped 5th and 95th percentile confidence intervals (CIs) confirm the statistical significance of this delay. In contrast, SEA detects no significant advance in the ED following major wildland fires, relative to the 3-year pre-fire average (Fig. 4b). This result also holds when applying alternative thresholds to define major fire events (Supplementary Fig. 11). Therefore, in the Arctic, the observed shortening of snow cover duration can be partially attributed to the substantial delay in snow cover formation in response to major wildland fires.

The delayed response of the SD to major wildland fires is not only significant but also positively correlated with the severity of wildland fires, as measured by BA. A generally positive relationship exists between SDs and BAs, with a regression slope close to 1.0 ($P < 0.1$), indicating that larger BAs lead to a later formation of snow cover. For example, the SD following a 4-Mha BA is about 3 days later than that following a 1-Mha BA, demonstrating that the delay in snow cover formation increases with fire severity (Fig. 4c). In contrast, the ED shows no significant correlation ($P > 0.1$) with fire severity (Fig. 4d). Thus, increased wildland fires in the Arctic lead to a significant delay in snow cover formation and this delay scales with fire severity.

Projections of BA and snow cover

The projections of BA were estimated using a least-squares linear multiple regression between the BA detected by AVHRR sensors (Fire-CCIv1.1) for 1982–2014 and the mean summer factors from CMIP6 models that were significantly related to BA during the same historical period (1982–2014). This multiple regression model was then applied to project the BA for the historical period (1950–2014) and the future period (2015–2100) under three scenarios: SSPs 2-4.5, 3-7.0 and 5-8.5 (Supplementary Table 2). For the projected annual snow cover duration, surface snow amounts from CMIP6 were used to calculate snow cover duration for both the historical period and three future scenarios.

The SSP 2-4.5, 3-7.0 and 5-8.5 scenarios indicate a substantial increase in BA in the Arctic (Fig. 5a). The annual BA under the SSP 2-4.5, 3-7.0 and 5-8.5 scenarios is projected to be 2.1, 2.4 and 2.6 times larger, respectively, than the historical average (Fig. 5b). Specifically, under the very high GHG emissions scenario (SSP 5-8.5), the BA could be in the range of 2.9–3.8 Mha in 2015, reaching 6.4–13.9 Mha by the end of this century (Fig. 5b). Comparisons of all ten models can be found in Supplementary Fig. 12. Conversely, the Arctic region is projected to experience a decrease in annual snow cover duration under all scenarios, reaching approximately 146 days, 137 days and 130 days by the end of this century under SSP 2-4.5, 3-7.0 and 5-8.5 scenarios, respectively (Fig. 5c). Furthermore, compared with the historical period, the annual mean snow cover duration under SSPs 2-4.5, 3-7.0 and 5-8.5 is projected to be 12 days, 15 days and 18 days shorter, respectively (Fig. 5d). Under the very high GHG emissions scenario (SSP 5-8.5), the annual mean duration of snow cover will be nearly a month shorter than in 2015 (159 days) by the end of this century. Comparisons across all

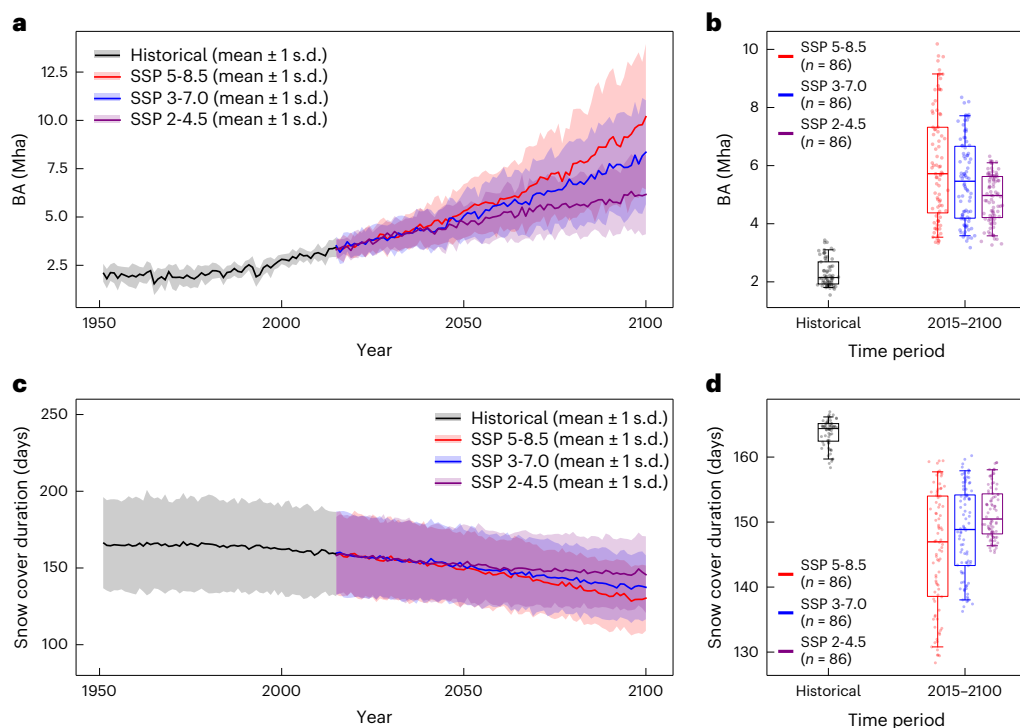


Fig. 5 | Projection of annual BA and snow cover based on CMIP6 models under three scenarios (SSPs 2-4.5, 3-7.0 and 5-8.5). **a**, Annual BA for the historical period (1950–2014) and the future period (2015–2100), including the SSP 2-4.5, 3-7.0 and 5-8.5 scenarios, in the Arctic region. **b**, Box plots of the annual BA during the periods of 1950–2014 and 2015–2100. **c**, Annual snow cover duration for the historical period (1950–2014) and the future period (2015–2100), including the

SSP 2-4.5, 3-7.0 and 5-8.5 scenarios, in the Arctic region. **d**, Box plots of the annual snow cover duration during the periods of 1950–2014 and 2015–2100. In **b** and **d**, the short horizontal line inside each box represents the 50th percentile (median), and the top and bottom edges of the box correspond to the 75th and 25th percentiles, respectively. The upper and lower ends of the whiskers indicate the 95th and 5th percentiles, respectively.

ten models are provided in Supplementary Fig. 13. Wildland fires and shortened snow cover will be exacerbated in a warming climate. In this context, the interaction between BA and snow cover may be amplified by climate change, greatly intensifying future wildland fires and further reducing snow cover beyond the effects of mean climate change alone. A shorter snow cover period can reduce forest ecosystem productivity and carbon sequestration, particularly in water-limited regions, where such dry conditions may also increase wildfire sensitivity as a result of higher solar radiation³¹.

Discussion

Our results indicate a substantial response of the delayed formation of snow cover to wildland fires. Meanwhile, the ED could also be influenced by wildland fires. For instance, the dust caused by wildfires in the Southern Rockies region increased the snow-free dates³², contributing to higher likelihood of snow drought³³. The dust deposition from wildland fires is particularly important during the snowmelt season. Dust layers over the snow surface lead to a reduction in surface albedo. This reduction in albedo underscores the importance of wildland fires on post-fire changes to snowmelt rate and timing^{34–36}. Consequently, wildland fires could also affect the snow cover duration through advancing the ED in different regions.

Our analysis focuses primarily on the response of snow cover to wildland fires. However, it is crucial to consider that the shortening of snow cover may also influence wildland fires. A shorter snow cover period contributes to prolonged exposure of the land to the effects of fire, intensifying the impact of wildland fires on the surrounding environment^{37,38}. This extended exposure can lead to increased surface heating and aridity, which in turn exacerbates the severity of BAs and contributes to the earlier arrival of the fire season (Supplementary Figs. 14 and 15). Understanding this relationship is vital for assessing

the potential risks and impacts of wildland fires on snow cover and for developing strategies to mitigate the effects of wildfires in regions with shortened snow cover duration.

The impacts of wildland fires on snow cover vary regionally. Factors such as terrain and climate variability also influence changes in snow cover from pre-fire to post-fire conditions. For instance, in some forest regions, trees intercept a portion of the snowfall before it reaches the ground; when trees burn, snow interception decreases. Since intercepted snow is more likely to sublimate back into the atmosphere^{39,40}, fires can lead to greater snowfall reaching the ground (that is, increased snow accumulation on the ground), thereby increasing the overall snow amount. Moreover, trees in forests also influence the wind redistribution of snow. Wind can scour snow from large, open areas, while small open areas surrounded by trees may retain more snow⁴¹. Therefore, forest clearing can either advance or delay the timing of snow-free conditions, depending on the terrain and the effects of wind redistribution⁴².

A shortened duration of snow cover affects not only the Arctic but also water-limited regions^{43–45}, potentially reducing forest ecosystem productivity and carbon sequestration⁴⁶. Such dry conditions may inhibit vegetation recovery after a fire, causing the impacts on snow cover to persist for decades⁴⁷. As a result, the response of snow cover to wildland fires is an increasingly pressing issue that requires global attention. As climate change continues to exacerbate these phenomena, studying the relationship between reduced snow cover and wildland fires is essential for predicting and managing their occurrence. By understanding the potential consequences of diminished snow cover resulting from wildfire activity, policy-makers, researchers and land managers can develop effective strategies to mitigate their cascading impacts. Furthermore, studying this response allows us to better understand the complex relationship between these two ecological disturbances, enabling the development of proactive measures to

break this linkage. Ultimately, recognizing the significance of the connection between reduced snow cover and frequent wildfires is crucial for protecting ecosystems, communities and biodiversity from the cascading effects of climate change.

Online content

Any methods, additional references, Nature Portfolio reporting summaries, source data, extended data, supplementary information, acknowledgements, peer review information; details of author contributions and competing interests; and statements of data and code availability are available at <https://doi.org/10.1038/s41558-025-02443-6>.

References

- Barnett, T. P., Adam, J. C. & Lettenmaier, D. P. Potential impacts of a warming climate on water availability in snow-dominated regions. *Nature* **438**, 303–309 (2005).
- Callaghan, T. V. et al. Multiple effects of changes in Arctic snow cover. *Ambio* **40**, 32–45 (2011).
- Bormann, K. J., Brown, R. D., Derksen, C. & Painter, T. H. Estimating snow-cover trends from space. *Nat. Clim. Change* **8**, 924–928 (2018).
- Brown, R., Marsh, P., Déry, S. & Yang, D. in *Arctic Hydrology, Permafrost and Ecosystems* (eds Yang, D. & Kane, D. L.) 61–99 (Springer, 2020).
- Groisman, P. Y., Karl, T. R. & Knight, R. W. Observed impact of snow cover on the heat balance and the rise of continental spring temperatures. *Science* **263**, 198–200 (1994).
- Flanner, M. G., Shell, K. M., Barlage, M., Perovich, D. K. & Tschudi, M. A. Radiative forcing and albedo feedback from the Northern Hemisphere cryosphere between 1979 and 2008. *Nat. Geosci.* **4**, 151–155 (2011).
- Evan, A. & Eisenman, I. A mechanism for regional variations in snowpack melt under rising temperature. *Nat. Clim. Change* **11**, 326–330 (2021).
- Stone, R. S., Dutton, E. G., Harris, J. M. & Longenecker, D. Earlier spring snowmelt in northern Alaska as an indicator of climate change. *J. Geophys. Res. Atmos.* **107**, ACL10-1–ACL10-13 (2002).
- Zhang, T. et al. Shifted sediment-transport regimes by climate change and amplified hydrological variability in cryosphere-fed rivers. *Sci. Adv.* **9**, eadi5019 (2023).
- Mankin, J. S., Viviroli, D., Singh, D., Hoekstra, A. Y. & Diffenbaugh, N. S. The potential for snow to supply human water demand in the present and future. *Environ. Res. Lett.* **10**, 114016 (2015).
- Wang, X. et al. Disentangling the mechanisms behind winter snow impact on vegetation activity in northern ecosystems. *Glob. Change Biol.* **24**, 1651–1662 (2018).
- Qin, Y. et al. Agricultural risks from changing snowmelt. *Nat. Clim. Change* **10**, 459–465 (2020).
- Ford, C. M., Kendall, A. D. & Hyndman, D. W. Effects of shifting snowmelt regimes on the hydrology of non-alpine temperate landscapes. *J. Hydrol.* **590**, 125517 (2020).
- Immerzeel, W. W., Van Beek, L. P. & Bierkens, M. F. Climate change will affect the Asian water towers. *Science* **328**, 1382–1385 (2010).
- Shindell, D. et al. Simultaneously mitigating near-term climate change and improving human health and food security. *Science* **335**, 183–189 (2012).
- Cayan, D. R. et al. Future dryness in the southwest US and the hydrology of the early 21st century drought. *Proc. Natl Acad. Sci. USA* **107**, 21271–21276 (2010).
- Musselman, K. N. et al. Projected increases and shifts in rain-on-snow flood risk over western North America. *Nat. Clim. Change* **8**, 808–812 (2018).
- Dennison, P. E., Brewer, S. C., Arnold, J. D. & Moritz, M. A. Large wildfire trends in the western United States, 1984–2011. *Geophys. Res. Lett.* **41**, 2928–2933 (2014).
- French, N. H. et al. Fire in Arctic tundra of Alaska: past fire activity, future fire potential, and significance for land management and ecology. *Int. J. Wildland Fire* **24**, 1045–1061 (2015).
- McCarty, J. L. et al. Reviews & syntheses: Arctic fire regimes and emissions in the 21st century. *Biogeosci. Discuss.* **2021**, 1–59 (2021).
- Chen, Y. et al. Future increases in Arctic lightning and fire risk for permafrost carbon. *Nat. Clim. Change* **11**, 404–410 (2021).
- Grabinski, Z. & McFarland, H. R. *Alaska's Changing Wildfire Environment 2.0* (Alaska Fire Science Consortium, 2025).
- Witze, A. Why Arctic fires are bad news for climate change. *Nature* **585**, 336–337 (2020).
- Pimentel, R. & Arheimer, B. Hydrological impacts of a wildfire in a Boreal region: the Västmanland fire 2014 (Sweden). *Sci. Total Environ.* **756**, 143519 (2021).
- Giovando, J. & Niemann, J. D. Wildfire impacts on snowpack phenology in a changing climate within the western US. *Water Resour. Res.* **58**, e2021WR031569 (2022).
- Kampf, S. K. et al. Increasing wildfire impacts on snowpack in the western US. *Proc. Natl Acad. Sci. USA* **119**, e2200333119 (2022).
- Smoot, E. E. & Gleason, K. E. Forest fires reduce snow-water storage and advance the timing of snowmelt across the Western US. *Water* **13**, 3533 (2021).
- Bliss, L. C. et al. Arctic tundra ecosystems. *Annu. Rev. Ecol. Evol. Syst.* **4**, 359–399 (1973).
- Chen, D. et al. Regional fire–greening positive feedback loops in Alaskan Arctic tundra. *Nat. Plants* **10**, 1886–1891 (2024).
- Heim, R. J. et al. Arctic tundra ecosystems under fire—alternative ecosystem states in a changing climate? *J. Ecol.* **113**, 1042–1056 (2025).
- Holden, Z. A. et al. Decreasing fire season precipitation increased recent western US forest wildfire activity. *Proc. Natl Acad. Sci. USA* **115**, E8349–E8357 (2018).
- Kaspari, S., McKenzie Skiles, S., Delaney, I., Dixon, D. & Painter, T. H. Accelerated glacier melt on Snow Dome, Mount Olympus, Washington, USA, due to deposition of black carbon and mineral dust from wildfire. *J. Geophys. Res. Atmos.* **120**, 2793–2807 (2015).
- Huning, L. S. & AghaKouchak, A. Global snow drought hot spots and characteristics. *Proc. Natl Acad. Sci. USA* **117**, 19753–19759 (2020).
- Sarangi, C. et al. Dust dominates high-altitude snow darkening and melt over high-mountain Asia. *Nat. Clim. Change* **10**, 1045–1051 (2020).
- Riihelä, A., Bright, R. M. & Anttila, K. Recent strengthening of snow and ice albedo feedback driven by Antarctic sea-ice loss. *Nat. Geosci.* **14**, 832–836 (2021).
- Usha, K. H., Nair, V. S. & Babu, S. S. Effects of aerosol-induced snow albedo feedback on the seasonal snowmelt over the Himalayan region. *Water Resour. Res.* **58**, e2021WR030140 (2022).
- Rogers, B. M., Soja, A. J., Goulden, M. L. & Randerson, J. T. Influence of tree species on continental differences in boreal fires and climate feedbacks. *Nat. Geosci.* **8**, 228–234 (2015).
- Kim, J. S., Kug, J. S., Jeong, S. J., Park, H. & Schaepman-Strub, G. Extensive fires in southeastern Siberian permafrost linked to preceding Arctic Oscillation. *Sci. Adv.* **6**, eaax3308 (2020).
- Gelfan, A. N., Pomeroy, J. W. & Kuchment, L. S. Modeling forest cover influences on snow accumulation, sublimation, and melt. *J. Hydrometeorol.* **5**, 785–803 (2004).
- Sextone, G. A. et al. Snow sublimation in mountain environments and its sensitivity to forest disturbance and climate warming. *Water Resour. Res.* **54**, 1191–1211 (2018).
- Broxton, P. D. et al. Quantifying the effects of vegetation structure on snow accumulation and ablation in mixed-conifer forests. *Ecohydrology* **8**, 1073–1094 (2015).
- Dickerson-Lange, S. E. et al. Snow disappearance timing is dominated by forest effects on snow accumulation in warm winter climates of the Pacific Northwest, United States. *Hydrol. Process.* **31**, 1846–1862 (2017).

43. Trujillo, E., Molotch, N. P., Goulden, M. L., Kelly, A. E. & Bales, R. C. Elevation-dependent influence of snow accumulation on forest greening. *Nat. Geosci.* **5**, 705–709 (2012).
44. Gleason, K. E. et al. Forest density intensifies the importance of snowpack to growth in water-limited pine forests. *Ecol. Appl.* **31**, e02211 (2021).
45. Huning, L. S. & AghaKouchak, A. Mountain snowpack response to different levels of warming. *Proc. Natl Acad. Sci. USA* **115**, 10932–10937 (2018).
46. Hu, J. I. A., Moore, D. J., Burns, S. P. & Monson, R. K. Longer growing seasons lead to less carbon sequestration by a subalpine forest. *Glob. Change Biol.* **16**, 771–783 (2010).
47. Coop, J. D. et al. Wildfire-driven forest conversion in western North American landscapes. *BioScience* **70**, 659–673 (2020).

Publisher's note Springer Nature remains neutral with regard to jurisdictional claims in published maps and institutional affiliations.

Open Access This article is licensed under a Creative Commons Attribution-NonCommercial-NoDerivatives 4.0 International License, which permits any non-commercial use, sharing, distribution and reproduction in any medium or format, as long as you give appropriate credit to the original author(s) and the source, provide a link to the Creative Commons licence, and indicate if you modified the licensed material. You do not have permission under this licence to share adapted material derived from this article or parts of it. The images or other third party material in this article are included in the article's Creative Commons licence, unless indicated otherwise in a credit line to the material. If material is not included in the article's Creative Commons licence and your intended use is not permitted by statutory regulation or exceeds the permitted use, you will need to obtain permission directly from the copyright holder. To view a copy of this licence, visit <http://creativecommons.org/licenses/by-nc-nd/4.0/>.

© The Author(s) 2025

Methods

Calculation of snow metrics and BAs

Supplementary Fig. 16 illustrates the terms used to describe the snow year. A snow year begins on 1 September of the current year and ends on 31 August of the following year. For instance, the 1990 snow year starts on 1 September 1990 and ends on 31 August 1991. Specifically, the start day (SD) of snow cover is defined as the first day, relative to 1 September, on which the SWE exceeds 10 mm and remains continuously above this threshold, marking the onset of snow cover formation. The annual snow cover duration is defined as the longest period of continuous snow cover (SWE > 10 mm) within a snow year. In cases with several periods of maximum duration, the earlier SD is used. The maximum SWE value during the longest period of continuous snow cover is defined as the peak SWE. The end day (ED) is defined as the last day, relative to 1 September, on which SWE exceeds 10 mm following the longest period of continuous snow cover (SWE > 10 mm), indicating the day when all snow has disappeared.

In evaluating wildland fires, we assessed the severity of wildland fires on the basis of the BA. Three satellite BA products were used, including MCD64A1 v.6 (ref. 48), FireCCI51 (ref. 49) derived from MODIS and the FireCCILT11 product⁵⁰ derived from AVHRR. FireCCI51 and MCD64A1 cover the period from 2001 to 2018, while FireCCILT11 spans from 1982 to 2018. Owing to its longer temporal coverage, all analyses of the relationship between wildland fire and snow cover are based on FireCCILT11. However, as FireCCILT11 does not provide data for 1994, all analyses exclude that year. Despite their utility, these fire products have several limitations. For instance, MCD64A1 exhibited a higher omission error in 2020 and FireCCILT11 is subject to known limitations such as orbit-drift artifacts, which may lead to overestimation of annual BAs before 2001. Nevertheless, FireCCILT11 captures the interannual variability observed in both FireCCI51 and MCD64A1 during the 2001–2018 period, with all three products showing an increase in BA during 2010–2018 compared with 2001–2009 (Supplementary Fig. 1). To ensure robustness, we repeated analyses using FireCCILT11 for the 2001–2018 period and consistently detected a delayed response in snow cover formation (Supplementary Fig. 17).

Analysis of historical trends

To evaluate long-term trends in BA and snow cover across the Arctic region, we performed a linear regression analysis using least-squares fitting⁵¹. Several candidate models, including linear, quadratic and exponential functions, were fitted and compared on the basis of their coefficients of determination (R^2). The linear model, which yielded the best fit, was selected for further interpretation. To quantify the uncertainty associated with the trend, we applied a non-parametric bootstrap procedure to generate 95% prediction intervals for the fitted curve⁵². The slope and its statistical significance (P value) were directly estimated using a standard linear regression approach⁵³.

Identification of factors influencing snow cover

Boosting trees refer to a decision tree-based machine learning approach. XGBoost enhances both the speed and predictive accuracy of gradient-boosted decision trees⁵⁴. In this study, we built and trained an XGBoost model to predict the delayed formation and early disappearance of snow cover using several environmental variables across pre-fire, during-fire and post-fire phases. These variables included albedo, LST, T_a , VPD, SW, LW and Def. These factors were selected on the basis of their relevance to both wildland fires and snow cover, as they are key to understanding snow accumulation and melt dynamics following fire events^{55,56}. In addition to these environmental variables, summertime BA, latitude and longitude were also considered. A binary cross-entropy loss function was applied in all XGBoost models. We generated a mesh of grid boxes with sizes of 4×4 ($1^\circ \times 1^\circ$), 8×8 ($2^\circ \times 2^\circ$) and 12×12 ($3^\circ \times 3^\circ$) across regions that experienced sustained summer wildland fires.

The response variables included delayed formation of snow cover (that is, SD deviating by >1 s.d. from the mean) and early disappearance of snow cover (that is, ED deviating negatively by >1 s.d. from the mean). The predictor features (pre-fire, during-fire and post-fire albedo, LST, T_a , VPD, SW, LW and Def, along with BA, latitude and longitude) were detrended and standardized (except for latitude and longitude). The during-fire phase refers to the month in which wildland fires occurred during summer, while the pre-fire and post-fire phases correspond to the 2 months preceding and following the fire month, respectively. This 2-month interval was selected on the basis of observed substantial differences in meteorological conditions between fire and non-fire years during these periods (Supplementary Fig. 18). As climatic anomalies during this transitional period can influence snowpack formation, we used the 2-month window for both pre- and post-fire phases. For each of the three phases, all predictor variables and response data were randomly divided into five equal-sized folds. The XGBoost was trained on four out of the five folds, with fivefold cross-validation applied internally on the training data to optimize hyperparameters—including the number of boosting rounds, maximum tree depth and column subsample ratio. The optimized model was then evaluated on the held-out one-fifth test fold. This process was repeated across all folds to assess the performance of the model in predicting delayed snow cover formation and early disappearance.

SHAP values are used in machine learning to interpret feature importance within a model. SHAP combines additive feature attribution methods with Shapley values from cooperative game theory, treating the prediction process as a cooperative game. Larger absolute SHAP values indicate a stronger impact on the predictions of the model, while negative (positive) values suggest a negative (positive) contribution. In this study, SHAP values were calculated using the TreeExplainer for XGBoost models to analyse the factors influencing the delayed formation and early disappearance of snow cover. This approach clarified the individual contribution of each factor and their interactions.

Causal analysis

To investigate the mechanisms by which wildland fires influence snow cover formation, we applied SEM, a statistical approach used to estimate causal relationships through both direct and indirect pathways^{57,58}. We hypothesized that the impact of wildland fires (that is, BA) on snow cover formation is mediated by changes in post-fire LST and post-fire albedo, which in turn influence post-fire T_a . The SEM included three mediating variables: post-fire LST, albedo and T_a . Path coefficients were estimated using maximum likelihood estimation.

To assess model performance, we calculated fit indices including the comparative fit index (CFI), Tucker–Lewis index (TLI), root mean square error of approximation (RMSEA) and standardized root mean square residual (SRMR). SEM was applied to grid meshes of 4×4 ($1^\circ \times 1^\circ$), 8×8 ($2^\circ \times 2^\circ$) and 12×12 ($3^\circ \times 3^\circ$) across regions with sustained summer wildland fires. All variables were standardized before analysis and we used the lavaan package in R (v.4.1.3) to estimate standardized path coefficients. Model adequacy was evaluated using commonly accepted thresholds: CFI ≥ 0.95 , TLI ≥ 0.95 , RMSEA ≤ 0.10 and SRMR ≤ 0.05 .

CCM⁵⁹ was used to test causal relationships between key variables, including summertime BA to post-fire LST, summertime BA to post-fire albedo, post-fire albedo to post-fire LST, post-fire LST to post-fire T_a and post-fire T_a to SD. CCM is a robust method for distinguishing causality from spurious correlations in nonlinear time-series systems. It detects causality by evaluating how well the historical record of a response variable (for example, SD) can estimate the state of a potential causal variable (for example, post-fire T_a). The strength of cross mapping is quantified by the correlation coefficient (ρ) between the predicted and observed values of the causal variable. An increasing ρ with longer time series and clear convergence indicates a causal effect. CCM was applied to annual time series of summertime BA, post-fire LST, post-fire albedo,

post-fire T_a , SD and ED across grid meshes of 4×4 ($1^\circ \times 1^\circ$), 8×8 ($2^\circ \times 2^\circ$) and 12×12 ($3^\circ \times 3^\circ$) in fire-affected regions. The analysis was conducted using the multispatial CCM package in R, with the optimal embedding dimension determined via simplex projection over the study period.

Superposed epoch analysis

SEA^{60,61} is a widely used method for analysing climate responses to extreme events. In this study, we extracted time-series data for regional annual snow cover duration, the SD and ED, to analyse their response to major wildland fires. We defined major wildland fire event years (year 0) as those with a BA of >1 s.d. above the mean, allowing for dating uncertainties of ± 3 years. We also tested other thresholds, including 0.8 and 1.2 s.d. above the mean. It is important to note that, since a snow year is defined from 1 September of the current year to 31 August of the following year (which differs from the fire year, calculated from 1 January to 31 December), our analysis of post-fire responses primarily focuses on year 0. This approach ensures that significant changes in snow cover duration in the latter part of the current snow year can be attributed to major wildland fires occurring earlier in the same year.

To assess significance, we generated a bootstrap sampling distribution by randomly drawing the same number of years as the major wildland fire events under consideration from the pool of non-major wildland fire years, repeating this process 1,000 times. For each draw, we calculated the composite using the same method applied to major wildland fire years. On the basis of these results, we determined the 5%, 10%, 90% and 95% quantiles of the non-major wildland fire years as the significance levels.

Projections of annual snow cover and BA

Projections of annual snow cover duration and BA were estimated using CMIP6 models for the historical period (1950–2014) and for three future scenarios—SSPs 2-4.5, 3-7.0 and 5-8.5—covering the years 2015 to 2100. The projected annual snow cover duration was derived from surface snow amounts ('snw') in CMIP6 for both the historical period and the three scenarios (SSPs 2-4.5, 3-7.0 and 5-8.5). For annual BA projections in the Arctic region, a two-step approach was used. First, a least-squares multiple linear regression was developed between the annual BA observed by the satellite product with the longest time span (FireCCI11, 1982–2014) and key related factors (that is, summer mean T_a and VPD). Second, related factors from CMIP6 were applied to this model to project annual BA for both the historical and future periods. Additionally, VPD was calculated from T_a and RH using data from CMIP6 models.

Data availability

All data supporting the findings of this study are openly available. The BA time series derived from AVHRR sensors (FireCCI11) is available at <https://doi.org/10.5285/62866635ab074e07b93f17fbf87a2c1a>. The BA time series derived from MODIS sensors are available at <https://doi.org/10.5067/MODIS/MCD64A1.006> for the MCD64A1 product and <https://doi.org/10.5285/58f00d8814064b79a0c49662ad3af537> for the FireCCI11 product. T_a (2-m air temperature), 2-m dewpoint temperature, potential evaporation and vegetation transpiration are available via ERA5-Land at <https://doi.org/10.24381/cds.68d2bb30> and VPD is calculated using the 2-m temperature and 2-m dewpoint temperature, while Def is calculated on the basis of potential evaporation and vegetation transpiration. These ERA5-Land variables are widely used and have demonstrated strong performance in previous studies^{62,63}. Furthermore, ERA5-Land offers higher spatial resolution, making it well suited for our analysis. The SWE is available at <https://data.tpdc.ac.cn/zh-hans/data/7a11f968-ef31-4b30-b7bf-b8c7471997c7>. Albedo, LST, SW and LW are derived from the Polar Pathfinder Extended Climate Data Record (<https://www.ncei.noaa.gov/products/climate-data-records/extended-avhrr-polar-pathfinder>). The CMIP6 models used for projecting snow cover and BA are available at <https://esgf-data.dkrz.de/>

[search/cmip6-dkrz/](https://github.com/qingyamin1/Delayed-formation-of-Arctic-snow-cover-in-response-to-wildland-fires-in-a-warming-climate). The data necessary to reproduce the main results are available via GitHub at <https://github.com/qingyamin1/Delayed-formation-of-Arctic-snow-cover-in-response-to-wildland-fires-in-a-warming-climate> (ref. 64).

Code availability

The computer code necessary to reproduce the main results is available via GitHub at <https://github.com/qingyamin1/Delayed-formation-of-Arctic-snow-cover-in-response-to-wildland-fires-in-a-warming-climate> (ref. 64).

References

- Giglio, L., Boschetti, L., Roy, D. P., Humber, M. L. & Justice, C. O. The Collection 6 MODIS burned area mapping algorithm and product. *Remote Sens. Environ.* **217**, 72–85 (2018).
- Lizundia-Loiola, J., Otón, G., Ramo, R. & Chuvieco, E. A spatio-temporal active-fire clustering approach for global burned area mapping at 250 m from MODIS data. *Remote Sens. Environ.* **236**, 111493 (2020).
- Otón, G., Lizundia-Loiola, J., Pettinari, M. L. & Chuvieco, E. Development of a consistent global long-term burned area product (1982–2018) based on AVHRR-LTDR data. *Int. J. Appl. Earth Obs.* **103**, 102473 (2021).
- Draper, N. R. *Applied Regression Analysis* (McGraw-Hill, 1998).
- Tibshirani, R. J. & Efron, B. *An Introduction to the Bootstrap* (Chapman and Hall, 1994).
- Helsel, D. R. & Hirsch, R. M. *Statistical Methods in Water Resources* (Elsevier, 1993).
- Nalluri, M., Pentela, M. & Eluri, N. R. A scalable tree boosting system: XG boost. *Int. J. Res. Stud. Sci. Eng. Technol.* **7**, 36–51 (2020).
- Descals, A. et al. Unprecedented fire activity above the Arctic Circle linked to rising temperatures. *Science* **378**, 532–537 (2022).
- Gottlieb, A. R. & Mankin, J. S. Evidence of human influence on Northern Hemisphere snow loss. *Nature* **625**, 293–300 (2024).
- Streiner, D. L. Finding our way: an introduction to path analysis. *Can. J. Psychiatry* **50**, 115–122 (2005).
- Rosseel, Y. lavaan: an R package for structural equation modeling. *J. Stat. Softw.* **48**, 1–36 (2012).
- Sugihara, G. et al. Detecting causality in complex ecosystems. *Science* **338**, 496–500 (2012).
- Haurwitz, M. W. & Brier, G. W. A critique of the superposed epoch analysis method: its application to solar-weather relations. *Mon. Weather Rev.* **109**, 2074–2079 (1981).
- Rao, M. P. et al. A double bootstrap approach to Superposed Epoch Analysis to evaluate response uncertainty. *Dendrochronologia* **55**, 119–124 (2019).
- Muñoz-Sabater, J. et al. ERA5-Land: a state-of-the-art global reanalysis dataset for land applications. *Earth Syst. Sci. Data* **13**, 4349–4383 (2021).
- Yilmaz, M. Accuracy assessment of temperature trends from ERA5 and ERA5-Land. *Sci. Total Environ.* **856**, 159182 (2023).
- Qing, Y., Wang, S., AghaKouchak, A. & Gentile, P. Delayed formation of Arctic snow cover in response to wildland fires in a warming climate. *GitHub* <https://github.com/qingyamin1/Delayed-formation-of-Arctic-snow-cover-in-response-to-wildland-fires-in-a-warming-climate> (2025).

Acknowledgements

The work described in this paper was partially supported by a grant from the Research Grants Council of the Hong Kong Special Administrative Region, China (project no. PolyU/RGC 15232023) and the Hong Kong Polytechnic University (project no. P0052737).

Author contributions

S.W. conceived of and supervised the study. Y.Q. and S.W. carried out the analysis and wrote the paper. A.A. and P.G. provided comments

and suggestions for improving the quality of this paper. Y.Q., S.W., A.A. and P.G. edited the paper.

Competing interests

The authors declare no competing interests.

Additional information

Supplementary information The online version contains supplementary material available at <https://doi.org/10.1038/s41558-025-02443-6>.

Correspondence and requests for materials should be addressed to Shuo Wang.

Peer review information *Nature Climate Change* thanks Michael Medler, Anne Nolin and the other, anonymous, reviewer(s) for their contribution to the peer review of this work.

Reprints and permissions information is available at www.nature.com/reprints.